JOURNAL OF SOLID STATE CHEMISTRY 12, 193–200 (1975)

# High Voltage Photovoltaic Effect in Barium Titanate and Lead Titanate–Lead Zirconate Ceramics*

P. S. BRODY

*Harry Diamond Laboratories, Washington, DC 20438*

Received July 3, 1974

Steady large photo-emf's proportional to length and remanent polarization were observed in the ceramic materials: $BaTiO_3$ + 5 wt% $CaTiO_3$, $Pb(Zr_{0.53}, Ti_{0.47})O_3$ with 1 wt% Nb, and hot pressed $Pb(Zr_{0.65}, Ti_{0.35})O_3$ with 7 and 8% lanthanum for lead substitutions. Photo-emf's are also dependent on material, grain size, and temperature. The large photo-emf's are shown to result from the addition of small emf's across individual ceramic grains. The smaller emf's are shown to be related to the spontaneous polarization of these grains. Short-circuit photocurrents were also observed as a function of intensity, temperature and illumination wavelength. The photocurrent vs photo-emf characteristics are shown to be approximated by an equivalent circuit consisting of a photo-emf in series with a photoresistance. The highest photo-emf, 1500 V/cm was observed in $Pb(Zr_{0.65}Ti_{0.35})O_3$ ceramic wafers with 2–4 $\mu$m grains. Largest short-circuit photocurrents, 0.31 $\mu A/cm/W/cm^2$, are observed in $Pb(Zr_{0.53}Ti_{0.47})O_3$ + 1 wt% Nb wafers, illuminated by band-gap light. In this last material, 0.02% of incident band-gap light is converted into electrical energy within a short-circuited sample.

## I. Introduction

The production of a high photo-emf in ceramics was first observed in the ceramic $BaTiO_3$ + 5 wt% $CaTiO_3$ (*1*). The effect has also been found in several other ferroelectric ceramics of the perovskite–oxide type (*3*). A photovoltaic effect in unpolarized ferroelectric ceramic had been found (*4*) to produce a much lower photo-emf. Low photo-emf's in single-crystal $BaTiO_3$ have also been seen (*5*, *6*). Possibly of similar origin to the photo-emf's in the ferroelectric ceramics and single crystals are photocurrents seen in $LiNbO_3$ single crystals, although in reality $LiNbO_3$ is not a true ferroelectric (*7*). High-voltage photo-emf's, though not previously reported in ferroelectrics, have been seen in other materials. Such an effect appears in films of evaporated semiconductors (*8*, *9*). It is believed that the much-greater-than-band-gap voltages produced in these films result from a situation in which accidental $p$–$n$ junctions occur at contacts between crystallites. Small photo-emf's at these junctions add up in series to produce the observed high photo-emf. A high-voltage photovoltaic effect has also been seen in insulating crystals of zinc sulfide by Merz and Ashkin et al. (*9*, *10*). This is also thought to be a multijunction effect. Stacking faults separating hexagonal and cubic modifications of the crystal have been suggested as the source of the small voltages. In these high-voltage effects, currents are small and both current and photo-emf are not particularly reproducible. The effect in the ceramics is, on the contrary, reproducible. A conversion efficiency in the ceramic material as high as 0.02% has been observed for band-gap light.

The production of photovoltages and photocurrents in both the ceramic and single-crystal ferroelectric materials depends on the photo excitation of carriers across the band gap. Photo excitation of carriers in ferroelectric ceramics is the source of another somewhat

* Invited paper.

related phenomenon—that of photoinduced refractive index changes—which has been investigated extensively. This effect was first observed by Ashkin et al. (*11*) in $LiNbO_3$ and has more recently been observed in ferroelectric ceramics (*12–14*). According to the investigators, the refractive index changes are an indirect manifestation of density gradients in photoinduced space charge. Electric fields produced by charge gradients affect the refractive index through the electrooptic activity typical of ferroelectrics. We have discovered that the high-voltage photovoltaic phenomenon is basically different. The electric fields are produced under uniform illumination and in a direction perpendicular to that in which the light is strongly absorbed. It is very likely an effect analogous to the barrier photovoltaic effect in single crystals, whereas the photoinduced refractive index changes are related to a gradient-produced bulk photovoltaic effect. In the new effect, these potential barriers occurring at grain boundaries produce small voltages at crystallite junctions that add up in series. For addition to occur in a polycrystalline material, both an axis and direction must be defined. The experimental results show that the spontaneous polarization within individual ceramic crystallites defines this axis and direction. This and other experimental results and their implications are described and discussed under appropriate headings in the succeeding subsections.

## II. Experimental Results and Discussion

### *(a) High-Voltage Photovoltaic Effect in Ferroelectric Ceramic. The Equivalent Circuit, Dependence on Length and Width, and Dependence on Intensity*

Photocurrent in ceramic materials flows through a circuit connecting electrodes when a polarized wafer of the ferroelectric ceramic (shown in Fig. 1) is uniformly illuminated over its entire surface.

To produce a current, the wafer must have been poled, that is, subjected to a high voltage across the electrodes. This voltage produces a remanent polarization (a net polarization at zero applied field) along *l*, the length of the wafer, in what was initially unpolarized ceramic. Once poled, the wafer need not be repoled except when the material has been depoled by bringing it above the Curie transition temperature of the particular material.

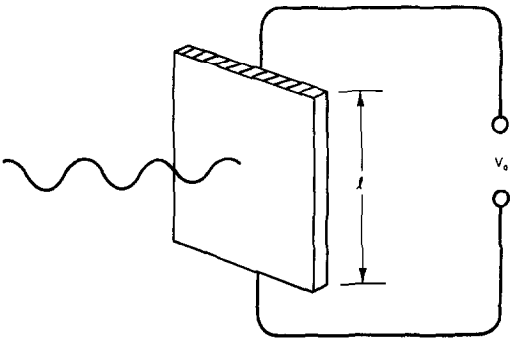


FIG. 1. An illuminated wafer. The shaded area is an electrode.

The wafer can be represented by an equivalent circuit consisting of a voltage in series with a high resistance. This is demonstrated by the results illustrated in Fig. 2, where an illuminated wafer was placed in series with a voltage source $V_a$ and an ammeter, as shown in Fig. 3. For this wafer, the open-circuit photo-emf, $V_0$, is 630 V (the intercept of the roughly straight line with the abscissa) and the short-circuit current, $i_{sc}$, $-0.31 \times 10^{-8}$ A (the intercept with the ordinate). The photoresistance, $R$, equal to $V/i$, is $2.2 \times 10^{11}$ Ω.

The relation between short-circuit current and intensity and photo-emf and intensity are both shown in Fig. 4. The results, which are for a particular material, are typical of

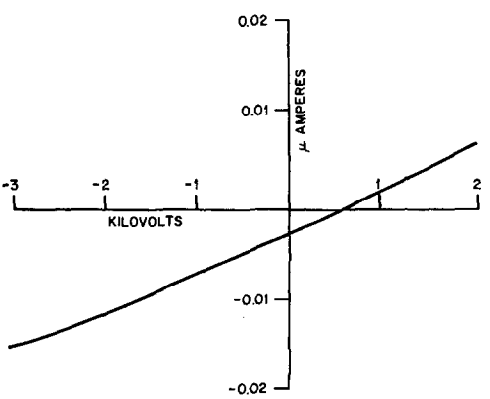


FIG. 2. Current vs applied voltages (illuminated wafer).

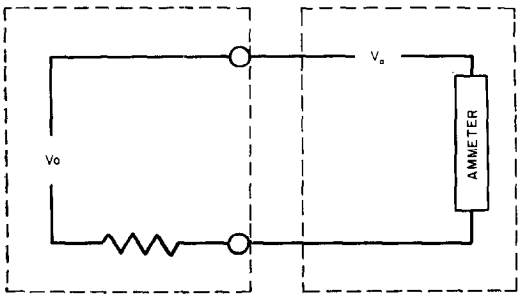


FIG. 3. Equivalent circuit (box to the left) and external circuitry used to make measurement shown in Fig. 2.

others. The short-circuit current is linear with intensity. The photo-emf is a function of intensity at low intensities, saturating at higher levels. The measurements of short-circuit current were made by using an electrometer as a feedback ammeter, with effectively zero potential drop across the measuring instrument. The photo-emf's are measurements of open-circuit voltage, made at effectively zero current and using a self-balancing potentiometric system. Illumination was the filtered flux from a high-pressure mercury arc. The illumination wavelength was roughly that of the band-gap energy. The measurements were made at constant temperature and thermal equilibrium to avoid the pyroelectric current which is proportional to the time rate of change of temperature. Illumination produces an initial pyroelectric current which then decays as the wafer comes to thermal equilibrium. A remaining steady-state current is the photovoltaic current. This steady current is always in the same direction as the pyroelectric current. It produces a voltage opposite in direction to that of the polarization.

The photo-emf is always proportional to the length $l$ of the wafer. This was shown by measurements made on wafers of different length. For a constant intensity of uniform illumination, the short-circuit current is independent of this length and proportional just to the wafer width. The photocurrent is usually independent of the thickness of the wafer because the current-producing illumination is absorbed in a distance that is small compared with the wafer thickness.

### (*b*) *Spectral Dependence of Ceramic Photocurrent and Photo-emf*

The charge carriers are injected into the conduction band, absorbing energy from incident photons. The short-circuit photocurrent thus is a function of wavelength, becoming large when the energy of the radiation exceeds the band gap, and then decreasing with increasing energy as more and more of the photons are absorbed closer to the surface. Experimental results of short-circuit photocurrent for barium titanate ceramic made using interference filters and a mercury high-pressure arc are shown in Fig. 5. One-half bandwidth

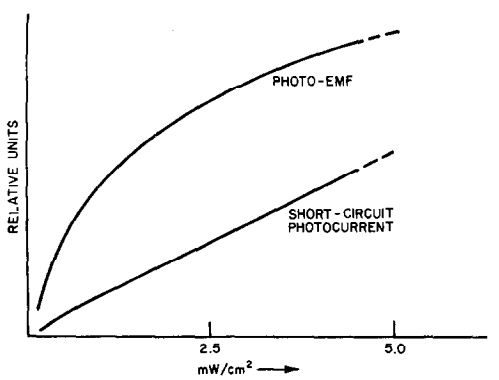


FIG. 4. Photo-emf and photocurrent as a function of intensity of illumination. These particular results are for a solid solution $Pb(Zr_{0.53}Ti_{0.47})O_3$ with about 1% more additives.

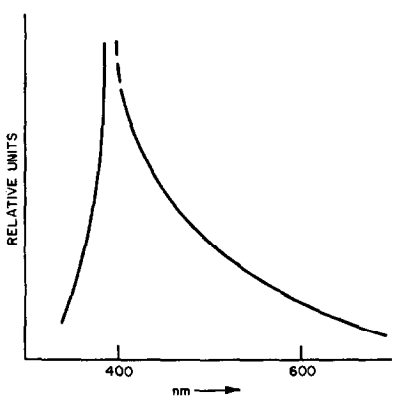


FIG. 5. Short-circuit photocurrent as a function of illumination wavelength for $BaTiO_3 + 5$ wt% $CaTiO_3$ ceramic.

for the filters was about 7 nm. Measurements were made at about constant intensity. Then, since photocurrent is a linear function of intensity, they were normalized to constant intensity.

The band gap for barium titanate has been determined at about 3 eV by Cox et al. (*15*). The photocurrent peak in Fig. 5 appears for photons of this energy.

Short-circuit photocurrent versus wavelength, measured in the same manner, is shown for two other ferroelectric ceramics in Figs. 6 and 7. The photocurrent vs wavelength results shown in Figs. 5, 6, and 7 have been smoothed somewhat, eliminating an undoubtedly valid fine structure—the source of which we do not understand clearly. The photo-emf was also a function of wavelength increasing with greater photon energy. This is shown for one of the materials in Fig. 8.

### (*c*) *Outputs for Different Materials*

In general, the output of a sample is well defined by designating the illumination (intensity and spectral distribution), a saturation photo-emf in V/unit length and short-circuit current ($i_{sc}$) in A/unit width. These quantities are shown for various materials in Table I.

The results in Table I are at room temperature and for fully poled material. Fully poled material is that material with saturated remanent polarization. In these cases, the poling voltage was applied until increasing the duration of application did not increase the remanent polarization (typically 20 min at room temperature for the lead titanate–lead zirconate solid solution).

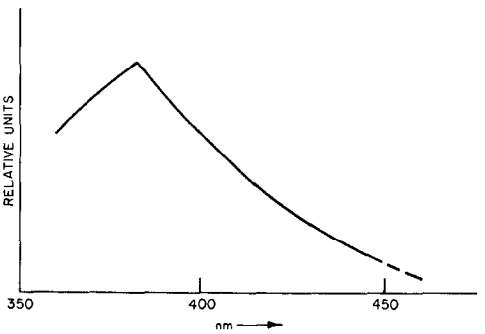


FIG. 7. Short-circuit photocurrent as a function of illumination wavelength for the solid solution $Pb(Zr_{0.65}Ti_{0.35})O_3$ with a 7% lanthanum–lead substitution.

### (*d*) *Dependence on Grain Size*

The dependence on wafer length suggests that as in the case of the evaporated semiconductor films and the zinc sulfide crystals, the high voltages are produced by a multijunction effect. The high photo-emf across a polycrystalline wafer results from the series addition of many small emf's across individual crystallites. Verification of the additive nature of individual grain photovoltage is found in the photo-emf's for ceramics of varying grain size. If small photo-emf's on individual grains add to produce a high photo-emf on a wafer, then the wafer's photo-emf must be linearly related to individual grain photo-emf by the

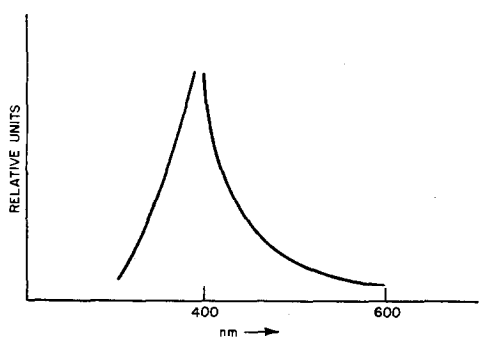


FIG. 6. Short-circuit photocurrent as a function of wavelength for the solid solution $Pb(Zr_{0.53}Ti_{0.47})O_3$ with about 1 wt% additional additive.

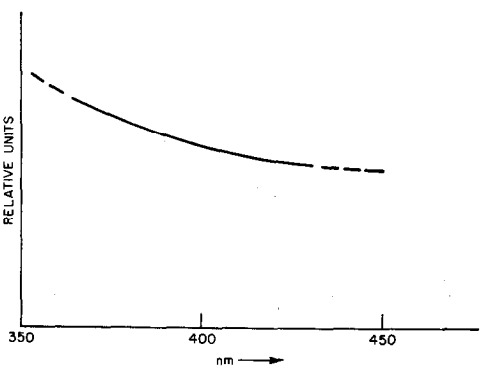


FIG. 8. Photo-emf vs wavelength of illumination for the solid solution, $Pb(Zr_{0.53}Ti_{0.47})O_3$ with about a 1 wt% additional additive.

TABLE I

PHOTOVOLTAIC OUTPUTS AT ROOM TEMPERATURE FOR SEVERAL CERAMIC COMPOSITIONS[a]

| Sample | Illumination wavelength (nm) | Saturation photo-emf (V/cm) | Short circuit photocurrent $\left(\frac{\mu A/cm}{W/cm^2}\right)$ |
|---|---|---|---|
| $Pb(Zr_{0.53}Ti_{0.47})O_3$ + 1 wt% NbO | 373 | 610 | 0.31 |
| $BaTiO_3$ + 5 wt% $CaTiO_3$ | 403 | 360 | 0.020 |
| $Pb(Zr_{0.65}Ti_{0.35})O_3$ 7% lanthanum–lead substitution | 382 | 1500 | 0.030 |
| $Pb(Zr_{0.65}Ti_{0.35})O_3$ 8% lanthanum–lead substitution | 382 | 750 | 0.015 |

[a] The wafers were fully poled. The $Pb(Zr_{0.53}Ti_{0.47})O_3$ material contained an additional additive of about 1 wt% NbO. Filtered illumination had a half bandwidth of about 7 nm. The photo-emf is a saturation value reached at a relatively low value of intensity.

inverse grain size following the relation for photo-emf ($V_0$),

$$V_0 = \phi_g l/lg, \tag{1}$$

where $l$ is wafer length, and $\phi_g$ is a small photo-emf appearing across a grain of average size $l_g$, and $\phi_g$ is assumed independent of grain size.

The relation, (Eq. 1) between photo-emf and inverse grain size was demonstrated by measurements of lead titanate–lead zirconate solid solutions with a lanthanum–lead substitution where the grain size could be controlled. Results for wafers of two somewhat different materials are shown in Table II. The approximately linear relation between photo-emf and inverse grain size is clear.

### (e) *Dependence on Remanent Polarization of Photo-emf*

The relation between remanent polarization and photo-emf was determined for barium titanate ceramic and is shown in Fig. 9. The wafer was illuminated by the direct radiation from a high-pressure mercury arc. The temperature of the thin (0.25 mm thick) wafer was stabilized by immersing it in silicone oil within an optical cell. The photo-emf was measured as before with a self-balancing

TABLE II

PHOTO-EMF FOR DIFFERENT GRAIN SIZE AND % LANTHANUM SUBSTITUTED FOR LEAD[a]

| Grain size ($\mu$m) | Lanthanum–lead substitution (%) | Saturation photo-emf (V/cm) |
|---|---|---|
| 2–4 | 7 | 1500 |
| 4–6 | 7 | 980 |
| >6 | 7 | 560 |
| 2–4 | 8 | 750 |
| 3–5 | 8 | 510 |
| 4–6 | 8 | 330 |
| >6 | 8 | 250 |

[a] The materials are $Pb(Zr_{0.65}Ti_{0.35})O_3$ with 7% lanthanum substitution for lead and the same material with an 8% lanthanum substitution for lead.

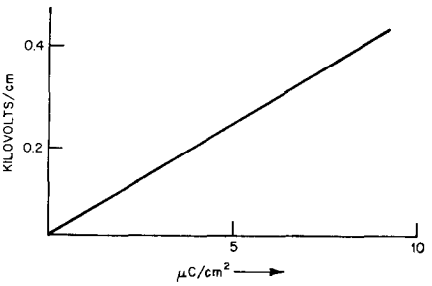


FIG. 9. Photovoltage vs remanent polarization, ceramic $BaTiO_3$ + 5 wt% $CaTiO_3$.

potentiometric system at zero current. A poling voltage limited in magnitude and duration was applied to produce a less-than-saturated remanent polarization in the wafer. The remanent polarization was measured by determining the charge released when the wafer was raised above the Curie transition temperature (thermally depoled).

The dependence of the photo-emf on the remanent polarization results from the alignment of domains of polarization. We assume that there is a photo-induced electric field in individual crystallites lying along the direction of the crystallite polarization (and directed oppositely in sign). In the unpoled material, the directions of spontaneous polarization of the crystallites are random. There is no net alignment. When poling voltage is applied, domains grow in the crystallites with polarization along the direction of the poling field. This configuration of domains remains after the poling voltage is removed. In poled material there is a net polarization (the remanent polarization) and a net photovoltage proportional to it. The components of polarization and photoinduced fields that are not aligned along the poling field cancel.

### (*f*) *Dependence on Temperature*

The photo-emf and the photocurrent vanish above the Curie transition temperature. At this temperature, ferroelectric materials go from a polar ferroelectric state in which axis and direction are defined to a nonpolar paraelectric state in which the crystal structure is centrosymmetric. An axis and direction is no longer defined and there can be no net alignment of crystallite photo-emf's, and therefore no photo-emf and no photocurrent. This is the situation observed experimentally. Photo-emf vs temperature is shown in Fig. 10 for barium titanate ceramic. Photocurrent and photo-emf were measured by methods similar to those used in obtaining the preceding results. The temperature of the cell could be controlled and held constant to within a small fraction of a degree.

The temperature dependence of the photo-emf below the transition temperature is probably related to the temperature dependence of the polarization and dielectric constant. The temperature dependence of the polarization ($P_r$) is shown also in Fig. 10. It was obtained by measuring the pyroelectric charge released as the temperature of the sample was raised by a method similar to that used to measure the remanent polarization. The temperature dependence of the polarization is not the result of a reduction in ordering of domains. This is demonstrated in Fig. 10, which shows that the results are reversible as long as the Curie temperature is not exceeded. It is rather the result of a dependence on temperature of the spontaneous polarization of individual domains. It is obvious, however, from the plotted results that the photo-emf does not simply follow the crystallite spontaneous polarization but is related to it in a more complicated way.

Short-circuit current vs temperature for barium–titanate ceramic is shown in Fig. 11. The increase and then decrease of the photocurrent with temperature (below the transition

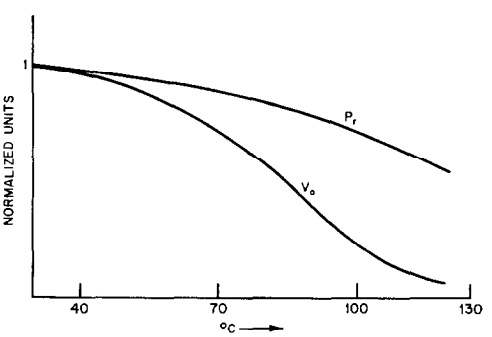


FIG. 10. Photovoltage and remanent polarization, $P_r$, vs temperature, ceramic $BaTiO_3$ + 5 wt% $CaTiO_3$.

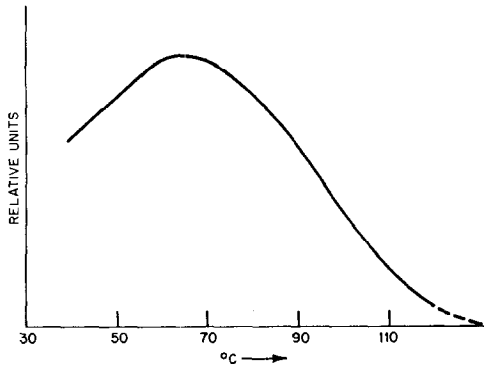


FIG. 11. Photocurrent vs temperature, $BaTiO_3$ + 5 wt% $CaTiO_3$.

temperature) is not surprising. Photocurrents in uniform photoconductors are commonly observed to both increase and decrease with increasing temperature, depending on the temperature range.

*(g) Single-Crystal Results*

The implication of the experimental results with the polycrystalline ferroelectrics is that photovoltages are produced in macroscopic single crystals and that they would appear across electrodes perpendicular to the spontaneous polarization axis of a single crystal. Of the polycrystalline materials examined, only barium titanate was available in single-crystal form. A photo-emf of 0.55 V at room temperature was observed across electrodes on the faces of a single crystal in the form of a parallelepiped. The electrodes were perpendicular to the polar axis. Visual observation and measurements of the anisotropic dielectric constant indicated that it was a single domain crystal. The arrangement is shown in Fig. 12. Photo-emf was measured as a function of temperature. The crystal

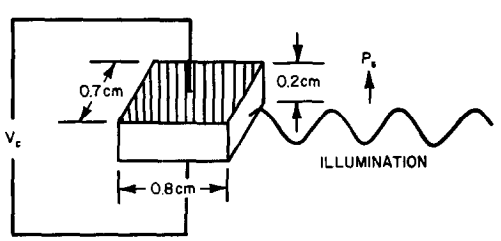


FIG. 12. Illuminated barium titanate single crystal.

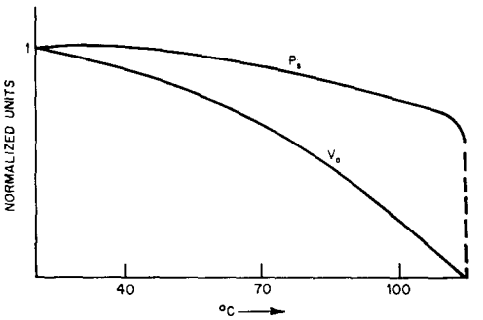


FIG. 13. Photovoltage and spontaneous polarization, $P_s$, vs temperature, $BaTiO_3$ single crystal.

was immersed in silicone oil within an optical cell. The photo-emf was measured with a vibrating capacitor electrometer, giving the results shown in Fig. 13. The emf decreases with increasing temperature. It vanishes above the transition temperature as would be expected from the polycrystalline results. The low value of the room temperature photo-emf supports the assumption previously made—that the photo-emf across a single grain is roughly the same as the 0.55 V appearing across the macroscopic crystal. Using the relationship, Eq. (1), with $\phi_g = 0.55$ V and $V_0$ (from Table I) = 350 V/cm, $l_g$ is calculated to be $1.6 \times 10^{-3}$ cm, which is in agreement with typical grain sizes given in the literature for stoichiometric barium titanate ceramic.

The spontaneous polarization vs temperature for the single crystal is also shown in Fig. 13. Notice the similarity of these curves to those for the polycrystalline material in Fig.

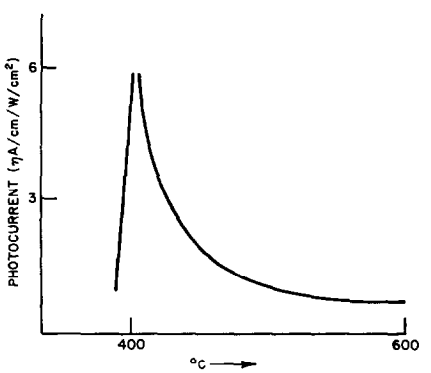


FIG. 14. Photocurrent vs wavelength for single crystal barium titanate.

10. The dependence on wavelength of the short-circuit photocurrent is shown in Fig. 14. The peaking at the band-gap wavelength is sharper than that obtained from the polycrystalline material.

## III. Conclusions

The high voltage photovoltaic in ferroelectrics is a new effect reminiscent perhaps of other high-voltage photovoltaic effects in that the high emf is produced by the series addition of smaller emf's. At present, we do not know the source of the smaller emf's although they appear clearly related to the spontaneous polarization of the material and have some barrier-like qualities. Considering these small emf's individually, in the materials examined they are less than the band-gap emf. Nevertheless, there is no particular indication that we are dealing with barriers produced by differences in Fermi level affected by crystallite polarization. Very possibly the fact that the photo-emf in the crystallite and single crystals we have examined is less than the band gap may be fortuitous—that is, not the result of a typical semiconductor barrier type mechanism.

The most significant observation at the moment is that the mechanism needed to produce net voltages in an initially disordered material is the ordering of spontaneous polarization domains. This is the first observation of such a situation. Nevertheless, we have observed the effect to some extent in all materials we have investigated, which are ferroelectric and polycrystalline. This class of materials has many members. Examination of these materials for high-voltage photovoltages should prove fruitful.

## Acknowledgments

The author gratefully acknowledges the contributions of HDL staff members, particularly James Blackburn for his helpful discussions and other assistance in developing instrumentation, also Stanley Watkins who made many of the measurements.

## References

1. P. S. BRODY, *Bull. APS* **18**, No. 1 (1973).
2. P. S. BRODY, *Solid State Commun.* **12**, 673 (1973).
3. P. S. BRODY, *Bull. Amer. Ceram. Soc.* **52**, 631 (1973).
4. P. S. BRODY AND M. J. VRABEL, *Bull. Amer. Phys. Soc.* **13**, 617 (1968).
5. A. G. CHYNOWETH, *Phys. Rev.* **102**, 705 (1956).
6. N. UCHIDA AND T. IKEDA, *Jap. J. Appl. Phys.* **7**, 1219 (1968).
7. F. S. CHEN, *J.A.P.* **40**, 3389 (1969).
8. L. PENSAK, *Phys. Rev.* **109**, 601 (1958).
9. J. TAUC, "Photo and Thermoelectric Effect in Semiconductors," Pergamon Press, London, 1962.
10. W. MERZ, *Helv. Phys. Acta* **31**, 625 (1958).
11. A. ASHKIN et al., *Appl. Phys. Letters* **9**, 72 (1966).
12. F. MICHERON, C. MAYEUX, A. HERMOSIN, AND J. NICOLAS, *Bull. Amer. Ceram. Soc.* **52**, 630 (1973).
13. F. MICHERON, C. MAYEUX, AND J. C. TROTTER, *Appl. Opt.* **13**, 784 (1974).
14. F. S. CHEN, J. T. LAMACCHIA, AND D. B. FRASER, *Appl. Phys. Letters* **13**, 223 (1968).
15. G. A. COX, G. G. ROBERTS, AND R. H. TREDGOLD, *Brit. J. Appl. Phys.* **17**, 793 (1966).